# REPORT DOCUMENTATION PAGE

AFRL-SR-BL-TR-00-

0414

Public reporting burden for this collection of information is estimated to average 1 hour per response, including the time for re gathering and maintaining the data needed, and completing and reviewing the collection of information. Send comments rega of information, including suggestions for reducing this burden to Washington Headquarters Service, Directorate for Informatio 1215 Jefferson Davis Highway, Suite 1204, Arlington, VA 22202-4302, and to the Office of Management and Budget, Paperwork Reduction Project (0704-0188) Washington, DC 20503.
PLEASE DO NOT RETURN YOUR FORM TO THE ABOVE ADDRESS.

| 1. REPORT DATE (DD-MM-YYYY) | 2. REPORT DATE | 3. DATES COVERED (From - To) |
|---|---|---|
| 17-08-2000 | Final | June 1996 - May 1999 |

**4. TITLE AND SUBTITLE**

AASERT-96 Growth and Nonlinear Optical Studies of Organic Single Crystal Films

**5a. CONTRACT NUMBER**

**5b. GRANT NUMBER**

F49620-96-1-0263

**5c. PROGRAM ELEMENT NUMBER**

**6. AUTHOR(S)**

Thakur, Mrinal

**5d. PROJECT NUMBER**

**5e. TASK NUMBER**

**5f. WORK UNIT NUMBER**

**7. PERFORMING ORGANIZATION NAME(S) AND ADDRESS(ES)**

Auburn University
310 Samford Hall
Auburn University, AL 36849

**8. PERFORMING ORGANIZATION REPORT NUMBER**

**9. SPONSORING/MONITORING AGENCY NAME(S) AND ADDRESS(ES)**

Air Force Office of Scientific Research
801 North Randolph St.
Arlington, VA 22203

**10. SPONSOR/MONITOR'S ACRONYM(S)**

AFOSR

**11. SPONSORING/MONITORING AGENCY REPORT NUMBER**

**12. DISTRIBUTION AVAILABILITY STATEMENT**

**DISTRIBUTION STATEMENT A**
**Approved for Public Release**
**Distribution Unlimited**

**13. SUPPLEMENTARY NOTES**

**14. ABSTRACT**

The objectives of this project include preparation and nonlinear optical studies of single-crystal films of specific organic materials. Large-area single crystal films of 4-aminobenzophenone (ABP) with a wide window of transparency and excellent optical quality have been prepared and characterized in detail. The cut-off wavelength of these films is at 390nm. The crystallographic orientation, and nonlinear optical susceptibilities of the films have been determined.

**15. SUBJECT TERMS**

| 16. SECURITY CLASSIFICATION OF: | | | 17. LIMITATION OF ABSTRACT | 18. NUMBER OF PAGES | 19a. NAME OF RESPONSIBLE PERSON |
|---|---|---|---|---|---|
| a. REPORT | b. ABSTRACT | c. THIS PAGE | | | Mrinal Thakur |
| | | | UU | 17 ~~16~~ | 19b. TELEPONE NUMBER (Include area code) 334-844-3326 |

Standard Form 298 (Rev. 8-98)
Prescribed by ANSI-Std Z39-18

DTIC QUALITY INSPECTED 4

# Growth and Nonlinear Optical Studies of Organic Single Crystal Films

**(AASERT)**

**(F49620-96-1-0263)**

M. Thakur, Auburn University

## Abstract

The objectives of this project include preparation and nonlinear optical studies of single-crystal films of specific organic materials. Large-area single crystal films of 4-aminobenzophenone (ABP) with a wide window of transparency and excellent optical quality have been prepared and characterized in detail. The cut-off wavelength of these films is at 390nm. The crystallographic orientation, and nonlinear optical susceptibilities of the films have been determined.

20000908 067



DTIC QUALITY INSPECTED 4

# Growth and Nonlinear Optical Studies of Organic Single Crystal Films

**(AASERT)**

**(F49620-96-1-0263)**

M. Thakur, Auburn University

## Final Report

The objectives of this project are to study crystal growth characteristics and nonlinear optical properties of important organic second order optical materials. We have studied specific organic materials having a broad transparency window. The material that we have studied in detail is 4-aminobenzophenone (ABP). Previous work on ABP by powder SHG test has indicated an efficiency of about 360 times that of ammonium dihydrogen phosphate (ADP). ABP has a monoclinic crystal structure, space group $P2_1$, unit cell parameters $a$ = 12.036, $b$ = 5.450, $c$ = 8.299 A, $\beta$ = 97.86°, and the number of molecules per unit cell $Z$ = 2.

Thin single-crystal films of ABP have been prepared by a modification of the shear method. This involves dissolving the material in a suitable solvent, placing the solution in the interface between two hydrophilic substrates, initiating the crystal growth by applying an initial shear in the interface, and then facilitating a slow evaporation of the solvent. The substrates were separated after the solvent evaporated completely, leaving single-crystal films on one of the substrates. Excellent optical quality single-crystal films (Figure 1) having areas of approximately 2 $cm^2$ were obtained on quartz substrates using this method. This is the first time that single-crystal thin films of ABP have been grown. Polarized optical microscopic observations proved the single crystal nature of the films. As the film was rotated under cross-polarized condition, two complete and uniform extinction directions in a cycle were observed, which correspond to the optical axes of the single crystal film. The thickness of the films was measured by a profilometer, and found to be 4 μm. The thickness was controllable within ~0.5 to 6 μm by controlling the pressure between the substrates during crystal growth.

X-ray diffraction (XRD) experiments were carried out to determine the crystallographic orientation of the single-crystal film. Figure 2 shows the XRD peaks, indicating [100] surface orientation parallel to the substrate. The orientation of the molecule on the plane of the substrate is given in Figure 3, which implies that the polar interaction between the carbonyl group of the molecule and the substrate is responsible for the growth of the single-crystal films of ABP. The charge transfer axis, pointing from the electron-donating amino group to the electron-accepting carbonyl group, lies close to parallel to the surface of the film. Figure 4 shows the orientation of the principal dielectric axes with respect to the crystallographic axes of ABP. The optical absorption spectra of the ABP thin film was measured by UV-visible spectroscopy using a U-2000 spectrophotometer (Figure 5). It has a broad window of transparency extending down to 390 nm, thus is suitable for blue light generation. The principal refractive indices, $n_X$, $n_Y$, and $n_Z$, for 1064 nm and 532 nm are listed in Table I, which were calculated from the Sellmeier's equation derived by Li et. al.

The nonlinear polarization induced in the medium by the optical electric field is dependent on the second-order polarizability matrix, constituted of the *d*-coefficients of the material. The nonzero elements of the nonlinear optical tensor for a monoclinic $P2_1$ crystal are $d_{14}$, $d_{16}$, $d_{21}$, $d_{22}$, $d_{23}$, $d_{25}$, $d_{34}$, and $d_{36}$, with $d_{14} = d_{25} = d_{36}$, $d_{16} = d_{21}$, and $d_{23} = d_{34}$ from Kleinman symmetry.

In our experiment the sample-film is rotated about the beam propagation direction. In order to obtain the second-harmonic intensity as a function of the film orientation angle, we define a film coordinate frame, $x'y'z'$, which is related to the fixed laboratory frame of reference, *xyz*, as shown in Figure 7. In this configuration the electric field and the induced nonlinear polarization vectors in the two coordinate frames are related through a rotational transformation. In the laboratory frame the nonlinear polarization is related to the electric field through the following equation:

$$\left(P_{2\omega}\right)_i = \sum_{jk} \sum_{lmn} a_{li} a_{mj} a_{nk} d_{lmn} E_j E_k \,, \tag{1}$$

where $a$'s represent the elements of the rotational transformation matrix, $d_{lmn}$ are the $d$-coefficients, and $E$'s are the components of the incident electric field vector.

For convenience, the incident beam is linearly polarized in the vertical direction, so that $E_Z$ is the only nonzero component. Thus, $\theta$ is also the angle between the incident optical electric field vector and the $z$ axis. Equation 1 leads to the final expressions for the in-plane components of the nonlinear polarization in the laboratory coordinate frame as the following:

$$P_y = 2\varepsilon_0\left(-d_{222}\sin\theta\cos^2\theta - d_{233}\sin^3\theta + 2d_{323}\sin\theta\cos^2\theta\right)E_z^2 = 2\varepsilon_0 d_{yzz}E_z^2, \quad (2)$$

$$P_z = 2\varepsilon_0\left(d_{222}\cos^3\theta + d_{233}\sin^2\theta\cos\theta + 2d_{323}\sin^2\theta\cos\theta\right)E_z^2 = 2\varepsilon_0 d_{zzz}E_z^2, \quad (3)$$

$$P_{eff} = 2\varepsilon_0\left(\sqrt{d_{yzz}^2 + d_{zzz}^2}\right)E_z^2 = 2\varepsilon_0 d_{eff}E_z^2, \quad (4)$$

where, the notation *yzz* implies that the propagation direction is along $x$ with the fundamental wave polarized parallel to $z$ and the second-harmonic wave polarized parallel to $y$, and *zzz* implies that the propagation direction is along $x$ with both fundamental and second-harmonic waves polarized parallel to $z$. Finally, the in-plane second-harmonic intensity, $I_i^{2\omega}$ (where $i$ stands for $y$, $z$, and *eff*), for a film of thickness $t$, has the following expression:

$$I_i^{2\omega} \propto \left(I_z^{\omega}\right)^2 d_i^2 t^2 \frac{\sin^2[\Delta kt/2]}{[\Delta kt/2]^2}, \quad (5)$$

where $\Delta k$ is the wave vector mismatch between the second-harmonic and the fundamental waves, and $I_Z^{\omega}$ is the intensity of the incident radiation. The equation is modified involving Fresnel coefficients and other terms in the case of a birefringent material.

The experimental setup used in the measurements of the second-harmonic intensity is shown in Figure 6. A mode-locked Nd:YAG laser, emitting 1064 nm beam at a repetition rate of 82 MHz, with a pulse-width of 100 ps, was used as the source of the fundamental radiation.

The power was attenuated to 4 W by employing a half-wave plate and a polarizer combination. The incident beam was mechanically chopped to synchronize with the detectors, and split into two arms by a beam-splitter to carry out measurements on the ABP film and a reference material simultaneously. After the beam passed through the nonlinear media, a harmonic beam splitter (HBS), having 99% reflectivity at 532 nm and 90% transmissivity at 1064 nm, was used to separate the second-harmonic beam from the fundamental wave. A set of color glass filters were placed before the photo-detector to remove the remaining fundamental beam from the SHG signal, and the second-harmonic intensity was measured by the lock-in detection technique.

The second-harmonic intensity was recorded as a function of the rotation of the sample about the beam propagation direction with three different polarization conditions:

(1) the output polarizer, $P_2$, parallel to the input polarizer, $P_1$, to measure the $z$-component of the second-harmonic intensity, $I_Z^{2\omega}$.

(2) $P_2$ perpendicular to $P_1$, to measure the $y$-component of the second-harmonic intensity, $I_y^{2\omega}$.

(3) without $P_2$, to measure the effective second-harmonic intensity, $I_{eff}^{2\omega}$.

Figure 7 shows the orientation of the crystal film on the beam axis, the direction of rotation of the crystal film, and the position of the input and output polarizers for different conditions. The experimental plots of $I_y^{2\omega}$, $I_Z^{2\omega}$, and $I_{eff}^{2\omega}$ as functions of the film orientation angle are shown in Figures 8($a$), 9($a$), and 10($a$), respectively. The calculated plots of $I_y^{2\omega}$, $I_Z^{2\omega}$, and $I_{eff}^{2\omega}$ are shown in Figures 8($b$), 9($b$), and 10($b$), respectively. The calculations were performed using Equations 2-5 with appropriate corrections due to birefringence.[12] The best agreement between the theoretical and experimental results was achieved with $d_{23}/d_{22}$=10.

In order to determine the absolute values of the $d$-coefficients of ABP, the results were compared with that of a reference material. A single-crystal thin film of 2-cyclooctylamino-5-nitropyridine (COANP), the nonlinear optical properties of which are known, was used in this experiment as the reference. Measurements of the effective second-harmonic intensity were done on a 6 μm thick film of COANP with the same setup as shown in Figure 6. The results were also verified by using a crystal of $LiNbO_3$ as the reference.

The thickness of the ABP single-crystal film was found to be less than the coherence length for any orientation of the film in the transverse configuration. Hence, the phase mismatch did not have any significant effect in depletion of the transfer of energy from the induced nonlinear polarization to the second-harmonic wave for propagation perpendicular to the film, which simplified the measurements. If the thickness of the film increases, the effect of phase mismatch needs to be taken into account, and thus second-harmonic intensity is changed. Figure 11 shows the effective second-harmonic intensity calculated as a function of the thickness and angle of rotation of the film about the propagation axis (using Eq. 5).

One of the most exciting advantages of the organic single-crystal thin film is that it can be used to fabricate waveguide structures with a well defined molecular orientation. In-plane propagation of the fundamental wave in the phase-matched direction would increase the interaction length by several orders of magnitude, thus enhance the second-harmonic generation (SHG) efficiency significantly. Refractive index data for the fundamental and second-harmonic frequencies have been analyzed to identify the phase-matched propagation directions in ABP film.

The refractive indices of ABP obey the following relations:

$$n_z^{2\omega} > n_z^{\omega} > n_y^{2\omega} > n_x^{2\omega} > n_y^{\omega} > n_x^{\omega}, \tag{6}$$

$$n_x^{2\omega} < \frac{1}{2}\left(n_x^{\omega} + n_z^{\omega}\right), \tag{7}$$

$$n_y^{2\omega} < \frac{1}{2}\left(n_y^{\omega} + n_z^{\omega}\right). \tag{8}$$

Hence, both type-I and type-II phase-matching should be possible in this material. The fundamental waves must have parallel polarizations in type-I, and orthogonal polarizations in type-II phase-matching schemes. Figure 12 shows the optical indicatrix surfaces for 1064 and 532 nm, and the phase-matched propagation directions on the *yz* and *xz* planes. The angles $\theta_1$ and $\theta_2$ indicate type-I, whereas $\phi_1$ and $\phi_2$ indicate type-II phase-matched propagation directions. $\theta_1$ represents the intersection of the refractive index surfaces at fundamental and second-harmonic frequencies on the *yz* plane, whereas intersection of the indicatrix surfaces at fundamental and second-harmonic frequencies on the *xz* plane gives $\theta_2$.

The results of the phase-match analysis for the fundamental wavelength of 1064 nm are summarized in Table II. ABP single crystal film has [100] surface orientation, thus the film lies in the *yz* plane. Directions for both type-I and type-II phase-matched propagation exist on the film-plane, along $\theta_1$ and $\phi_1$, respectively. Hence, it should be possible to fabricate single-crystal planar and channel waveguides on the ABP films that will allow phase-matched second-harmonic generation.

Analysis of Equation 5 shows that the maximum absolute value of $d_{eff}$ of ABP is obtained at $\theta$=90°, and is equal to the magnitude of $d_{23}$. The value of $(d_{eff})_{max}$ of ABP was determined by comparing the effective second-harmonic intensity of ABP to that of COANP, taking into account the Fresnel coefficients to incorporate the effect of birefringence of the film.[12] Consideration of the effect of birefringence, however, led to only about 1.4% change in the magnitude of the *d*-coefficient because of the thin crystal and the experimental configuration used. The maximum value of $d_{eff}$ of COANP can be shown to be equal to $d_{32}$, and was reported to be 56 pm/V. The maximum value of $d_{eff}$ of ABP was found to be equal to 7.3±0.4 pm/V. The results were also checked using a $LiNbO_3$ crystal as the reference. The best match between the theoretical and experimental results was obtained for $d_{22}/d_{23}$=0.1. Thus, the magnitudes of the substantial elements of the second-order polarizability tensor for ABP at the fundamental wavelength of 1064 nm were determined as: $d_{23}$=7.3±0.4 pm/V, and $d_{22}$=0.73±0.04 pm/V.

As mentioned earlier, there exists a strong charge transfer interaction along the twofold rotational axis of the benzene ring in the ABP molecule due to the presence of electron-donor and electron-acceptor substituents, amino and carbonyl group, respectively. The direction along the polar axis should be the most polarizable, which is validated by the fact that $d_{23}$ was found to be the largest *d*-coefficient. The value of $d_{eff}$ is larger than that reported earlier (6.8 pm/V). The bulk crystal used in that work was reported to have poor polishing of the surfaces, resulting in substantial scattering losses. These losses have largely been avoided in the present work due to good optical quality single-crystalline films.

The measurements were simplified due to the fact that the thickness of the single-crystal film was less than the coherence length for any angular orientation under the transverse

configuration, with the beams propagating perpendicular to the film. As the thickness of the film increases, phase mismatch leads to alteration of the second-harmonic intensity. The optimum thickness of ABP single-crystal film for transverse SHG measurements can be determined from Figure 11. Clearly, these films are suitable for phase-matched frequency conversion at shorter wavelengths using the waveguide geometry..

Studies of another material, 8-(4'-acetylphenyl)-1,4-dioxa-8-azaspiro[4.5]decane (APDA), has been initiated. The preliminary results indicate potential for preparation of large-area single-crystal films. This material will be studied in detail in future research.

Table I. Angles for phase-matched propagation directions in the single-crystalline thin films of ABP.

| TYPE-I | | TYPE-II | |
|---|---|---|---|
| yz-plane | xz-plane | yz-plane | Xz-plane |
| $\theta_1$=67.37° | $\theta_2$=60.82° | $\phi_1$=55.96° | $\phi_2$=48.87° |

**Students Involved:**

Two graduate students, Rupa Raju and Nicole Faulk, were supported in this project.

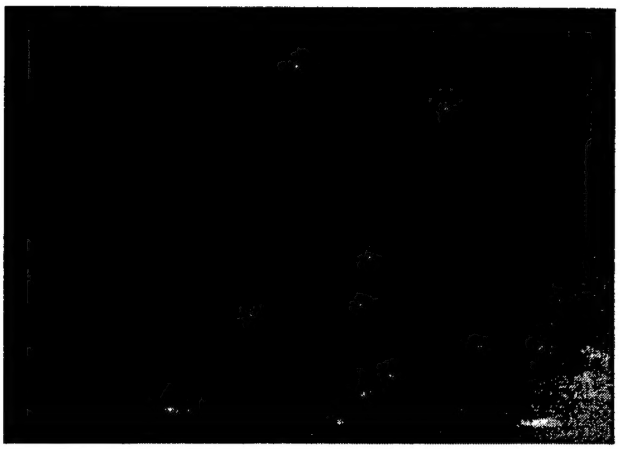

Fig. 1. Micrograph of single-crystal thin film of ABP obtained from polarized optical microscopy.

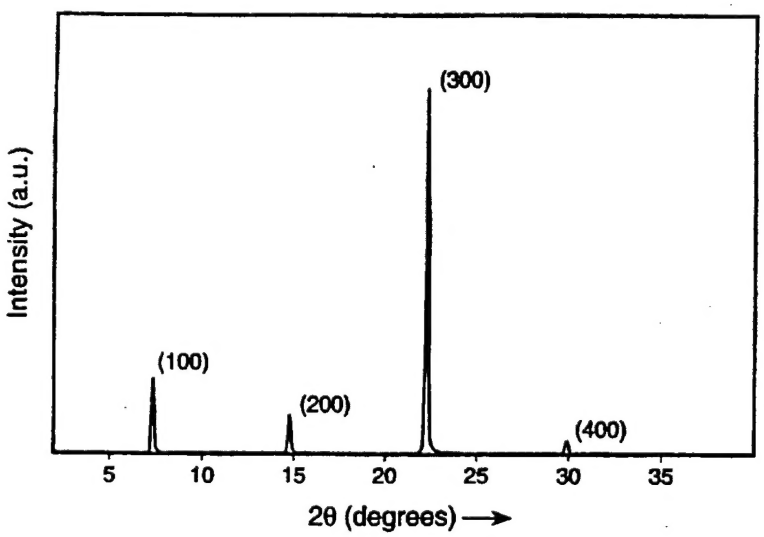


Fig. 2. X-ray diffraction peaks obtained from ABP single-crystal films. The film surface corresponds to the *yz* crystallographic plane.

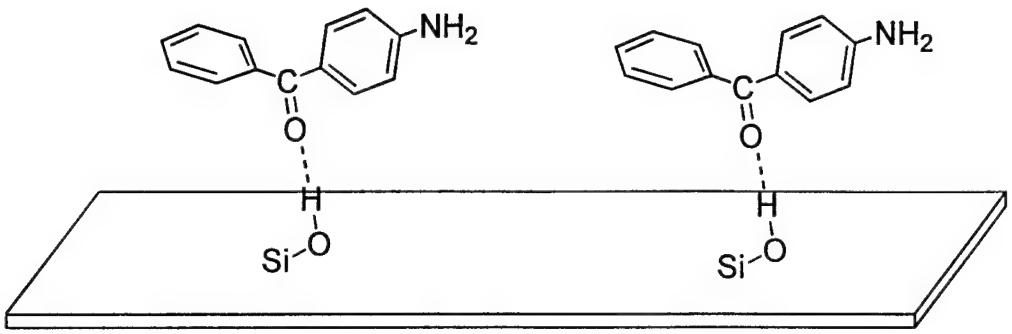


Fig. 3. Orientation of the ABP molecule on the plane of the single-crystal film.

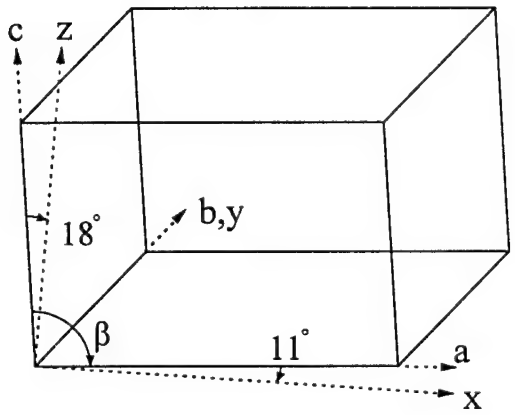


Fig. 4. Relationship between the crystallographic axes and the principal dielectric axes of ABP crystal.

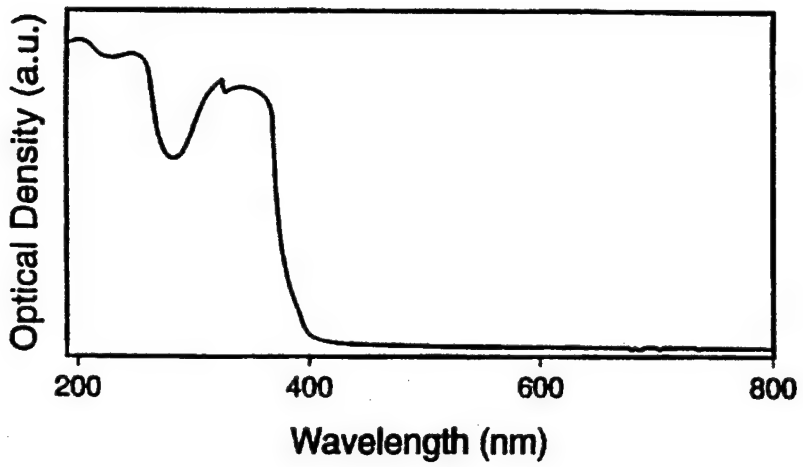


Fig. 5. Optical absorption spectra of ABP single-crystalline thin film measured by a UV-visible spectrophotometer. The cut-off is at ~390 nm.

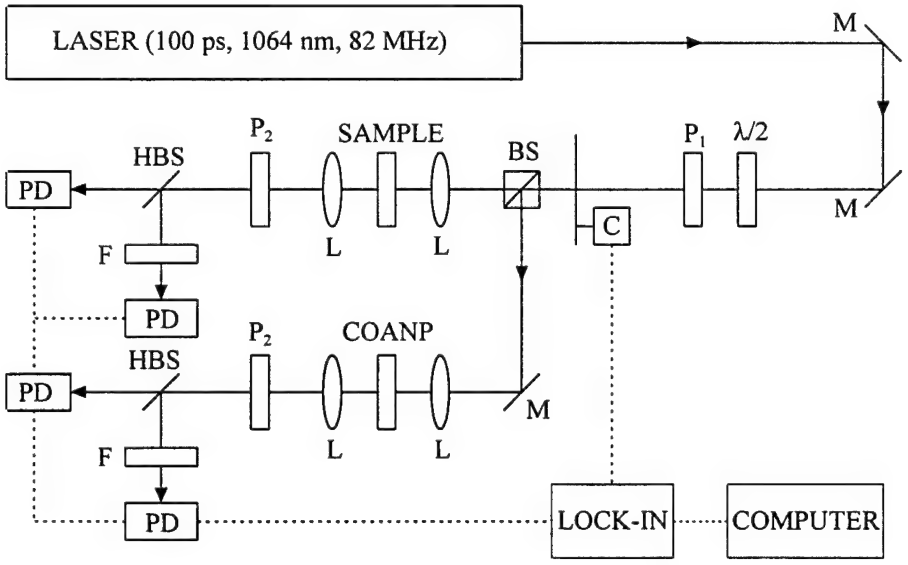


Fig. 6. Experimental setup used in SHG measurements. Ms, mirror; λ/2, half-wave plate; Ps, polarizer; C, optical chopper; Ls, lens; HBSs, harmonic beam splitter; Fs, filter; PDs, photodetector; and LOCK-IN, lock-in amplifier.

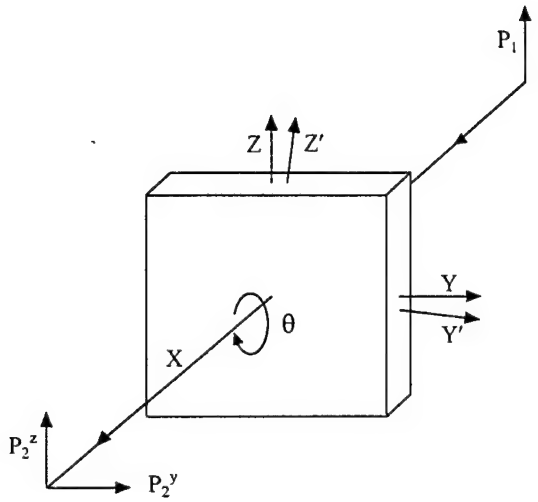


Fig. 7. Configuration of the sample and polarizers. *xyz*, fixed laboratory frame of reference; *x y′z′*, rotating film coordinate frame. The sample is rotated about the beam propagation (*x*) axis. $P_1$, input polarizer; $P_2^y$ and $P_2^z$, output polarizers, used to measure the *y*- and *z*-components of the SHG intensity, respectively.

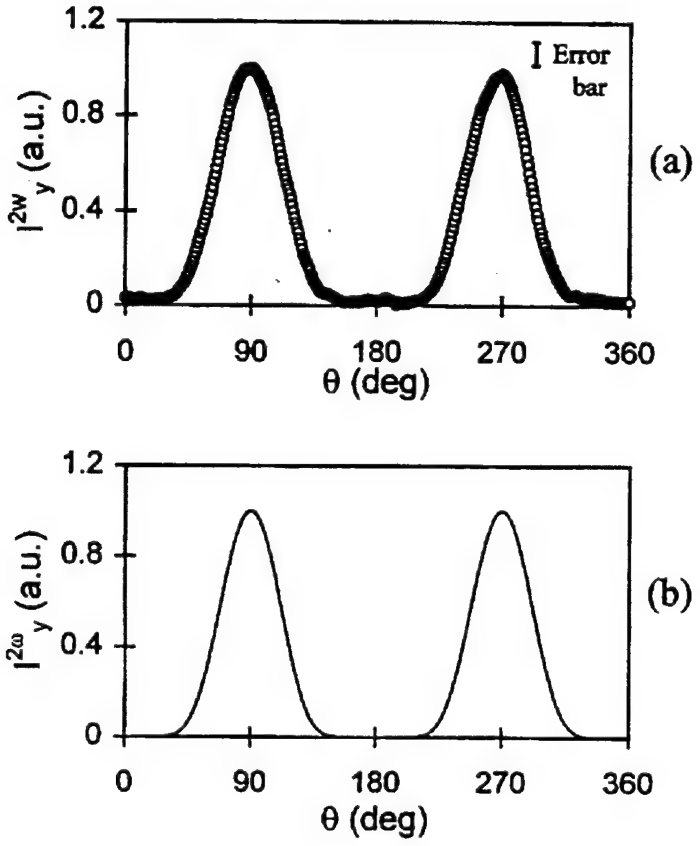


Fig. 8. Second-harmonic intensity with cross-polarized configuration as a function of the angular position of the crystal film with respect to the input polarization. (a) Experimental results, (b) Theoretical curve.

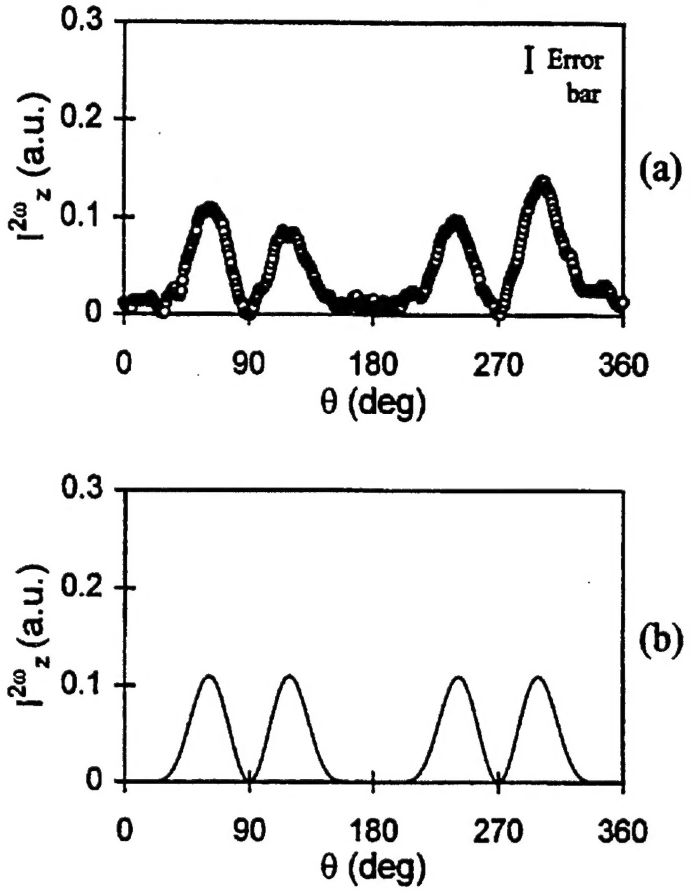


Fig. 9. Second-harmonic intensity with the input and output polarizers parallel to each other as a function of the angular position of the crystal film with respect to the input polarization. (a) Experimental results, (b) Theoretical curve.

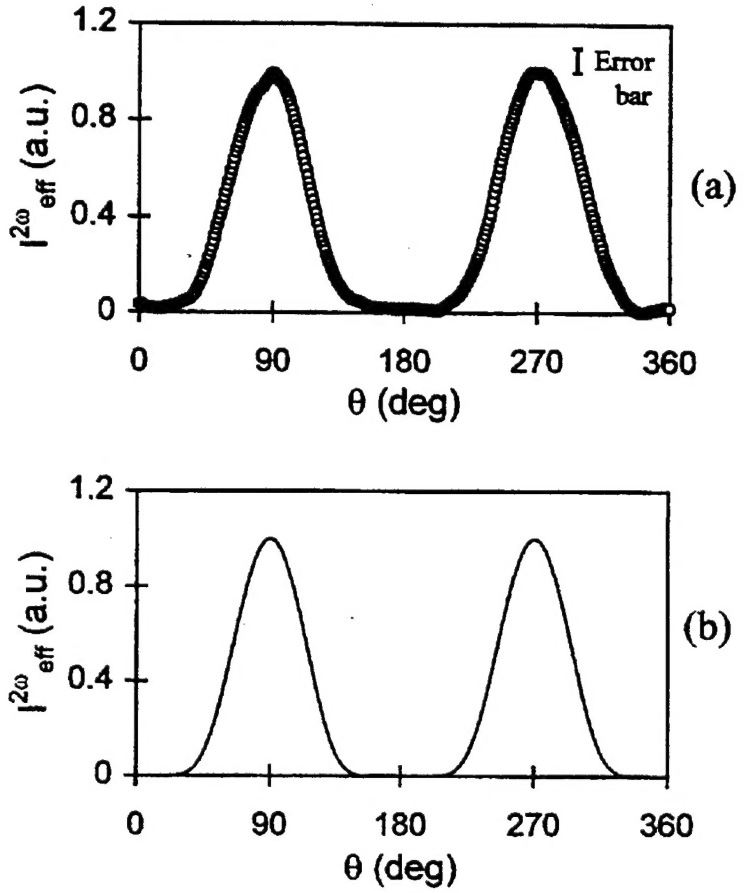


Fig. 10. Effective second-harmonic intensity as a function of the angular position of the crystal film with respect to the input polarization. (a) Experimental results, (b) Theoretical curve.

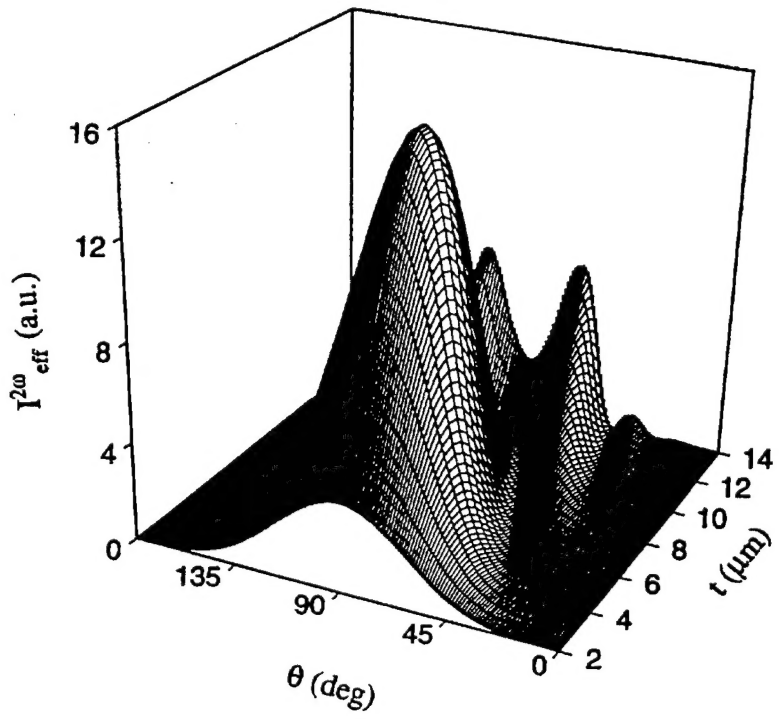


Fig. 11. Effective second-harmonic intensity theoretically calculated as a function of the thickness and the angular position of the crystal film with respect to the input polarization. SH intensity is depleted due to phase mismatch if the thickness of the film exceeds the coherence length.

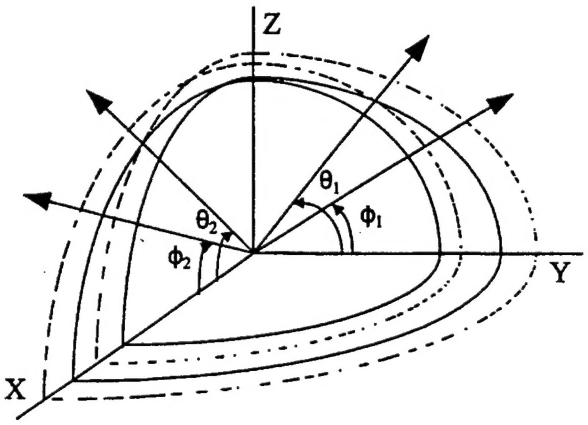


Fig. 12. Optical indicatrix (refractive index) surfaces for ABP, and the phase-matched propagation directions. $\theta_1$ and $\theta_2$ represent type-I, $\phi_1$ and $\phi_2$ represent type-II phase-matching. The continuous and dashed lines represent 1064 and 532 nm, respectively.